Journal of Power Sources 215 (2012) 43–47

Contents lists available at SciVerse ScienceDirect

Journal of Power Sources

journal homepage: www.elsevier.com/locate/jpowsour

Short communication

Carbon nanotubes/cobalt sulfide composites as potential high-rate and high-efficiency supercapacitors

Chia-Ying Chen, Zih-Yu Shih, Zusing Yang, Huan-Tsung Chang*

Department of Chemistry, National Taiwan University, 1, Section 4, Roosevelt Road, Taipei 106, Taiwan

HIGHLIGHTS

- The annealed CNT/CoS composites provide 2140 ± 90 F g^{-1} for specific capacitance.
- CNT/CoS composites yield high-power density at a current density of 217.4 A g^{-1}.
- CNT/CoS supercapacitors demonstrate great potential as energy storage devices.

GRAPHICAL ABSTRACT

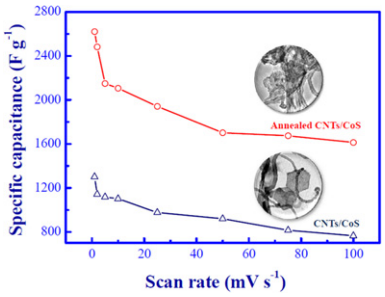

ARTICLE INFO

Article history:
Received 29 December 2011
Received in revised form
12 March 2012
Accepted 26 April 2012
Available online 10 May 2012

Keywords:
Supercapacitors
Cobalt sulfide
Nanomaterials
Carbon nanotubes
Energy storage

ABSTRACT

We have prepared carbon nanotube (CNT)/cobalt sulfide (CoS) composites from cobalt nitrate, thioacetamide, and CNTs in the presence of poly(vinylpyrrolidone). CNT/CoS composites are deposited onto fluorine-doped tin oxide glass substrates and then subjected to simple annealing at 300 °C for 0.5 h to fabricate CNT/CoS electrodes. Data collected from Raman spectroscopy, X-ray photoelectron spectroscopy, high-resolution transmission electron microscopy, and *d*-spacing reveal the changes in the CoS structures and crystalline lattices after annealing. Cyclic voltammetry results reveal that the annealed CNT/CoS composite electrodes yield values of 2140 ± 90 and 1370 ± 50 F g^{-1} for specific capacitance at scan rates of 10 and 100 mV s^{-1}, respectively. To the best of our knowledge, the annealed CNT/CoS composite electrodes provide higher specific capacitance relative to other reported ones at a scan rate of 100 mV s^{-1}. CNT/CoS composite electrodes yield a power density of 62.4 kW kg^{-1} at a constant discharge current density of 217.4 A g^{-1}. With such a high-rate capacity and power density, CNT/CoS composite supercapacitors demonstrate great potential as efficient energy storage devices.

1. Introduction

Electrochemical capacitors also known as supercapacitors (SCs) or ultracapacitors possess unique electrochemical capacity characteristics, such as high energy and power densities and long cycle life, which make them promising for the fabrication of highly efficient energy storage devices [1–3]. With the recent advances in nanotechnology, many cost-effective SCs of $NiCo_2O_4$, MnO_2, and graphene have been prepared [4–7]. Because these low-cost nanomaterials (NMs) provide high capacitances up to 760 F g^{-1}, they are good candidates to replace the currently used expensive SCs like RuO_2 [8–10]. However, preparation of ideal and cost-effective SCs that provide high capacitance (>2000 F g^{-1}) and high energy and power densities (>15 kW kg^{-1}) remains challenging [11–13].

Integration of metal or metal oxide NMs with one-dimensional carbon nanotubes (CNTs) has been shown to be effective for enhancing specific capacitance [14–17]. For example, CNT/MnO_2,

* Corresponding author. Tel./fax: +886 2 33661171.
E-mail address: changht@ntu.edu.tw (H.-T. Chang).

0378-7753/$ – see front matter Crown Copyright © 2012 Published by Elsevier B.V. All rights reserved.
doi:10.1016/j.jpowsour.2012.04.075

CNT/Co_3O_4, and CNT/NiO_x electrodes yield capacitance values of 944, 1066, and 1701 F g^{-1} [18–24]. Such high capacitance values generated are mainly due to spatial confinement and synergetic electronic interactions between metal oxides and CNTs [25–28]. CNT/NM composites have three-dimensional network structures, which provide high electrical conductivity and efficient ionic transport throughout the internal volume of the electrode [18–22]. These CNT/NM composite electrodes are commonly prepared by a spontaneous direct redox reaction between CNTs and metal oxide precursors; the precursors are adsorbed on the surfaces of CNTs and then form metal oxides by the decomposition or redox reaction under thermal conditions [18–22].

Our study is focused on the characterization and electrochemical tests of CNT/CoS composites for SCs applications. These composites can be simply prepared from cobalt nitrate ($Co(NO_3)_2$), thioacetamide, and CNTs in the presence of poly(vinylpyrrolidone) (PVP). Aliquots of the as-prepared CNT/CoS composites solution were deposited onto fluorine-doped tin oxide (FTO) glass substrates and were annealed at 300 °C for 0.5 h. The as-prepared CNT/CoS composite electrodes ($n = 10$) provided extremely high specific capacitance up to 2140 ± 90 F g^{-1}, demonstrating their great potential as new-generation SCs.

2. Experimental

2.1. Materials

Commercially available $Co(NO_3)_2$, CNTs, EtOH, KOH, Nafion, NaOH, PVP (M_w 55,000), and thioacetamide were purchased from Sigma–Aldrich (Milwaukee, WI, USA). 20 μm thick Surlyn® resins were purchased from DuPont (Taipei, Taiwan).

2.2. Preparation of CNT/CoS NMs

$Co(NO_3)_2$ (0.116 g), thioacetamide (0.05 g), CNTs (0.01 g), and PVP (0.014 g) were added to ultrapure H_2O (final volume: 10 mL) in a glass bottle. After addition of NaOH (0.5 M, 2.4 mL), the solution was heated at 100 °C for 60 min. The color of the mixture became black, indicating the formation of CNT/CoS NMs. The CNT/CoS NM solution was subjected to sonication for at least 60 min and then to two centrifugations (6000 rpm, 10 min)/wash (EtOH, 2 × 15 mL). CNT/CoS composites were then redispersed in EtOH (1.0 mL) prior to use.

2.3. Preparation of CNT/CoS NM electrodes and SCs

Droplets (2 μL) of the dispersed CNT/CoS NMs solution (2.3 mg in 1 mL of EtOH) were placed on the solid surfaces of FTO substrates, each having an effective area of 1 cm^2. The electrodes were then dried in an oven at 100 °C for 10 min. Some CNT/CoS composite electrodes were further annealed in the oven at 300 °C for 0.5 h. The as-prepared CNT/CoS composite electrodes were characterized and used as SCs. In order to construct a symmetric SC, two CNT/CoS composite electrodes prepared under similar experimental conditions from a same batch were used. In a typical procedure, a symmetric SC was fabricated by mounting a 20 μm thick Surlyn resin on one of the CNT/CoS composite electrodes in a fashion that three sides were kept closed while one side was left open. Then, another composite electrode was placed on the resin and heated in an oven at 100 °C for 10 min to fix both the electrodes firmly. Finally, the as-fabricated SC was allowed to cool at room temperature and 1 M KOH was injected into the mounted cell until all air was replaced.

2.4. Measurements

Transmission electron microscopy (TEM) images were recorded using a JEOL JSM-1230 instrument (Hitachi, Tokyo, Japan). A TEM system (Tecnai 20 G2 S-Twin, Philips, OR, USA) was used to record high-resolution TEM (HRTEM) images. Cyclic voltammetry (CV), and galvanostatic charge–discharge measurements were performed using an electrochemical analyzer (CHI 802A, CH Instruments, Austin, TX). The electrolyte used in these measurements was 1 M KOH. A three-electrode configuration was employed in the CV measurements of the CNT/CoS composite electrodes (effective area: 1.0 cm × 1.0 cm): a CNT/CoS composite electrode or a symmetric SC consisting of two CNT/CoS composite electrodes as a working electrode, Pt counter electrode, and saturated calomel electrode (SCE) as a reference electrode. X-ray photoelectron spectroscopy (XPS) spectra were recorded using a hemispherical energy analyzer 100 (SPECS, Berlin, Germany). The main peak in carbon 1s XPS spectra was considered as a reference.

3. Results and discussion

Fig. S1 depicts TEM images of CNT/CoS composites before (Fig. S1A–C) and after (Fig. S1D–F) thermal annealing at 300 °C for 0.5 h. The TEM image depicted in Fig. 1A clearly displays that there are some CoS hexagonal nanostructures attached to the CNTs. From the magnified TEM image (Fig. S1B), we estimated from 300 counts that the sizes of CoS hexagonal nanostructures are 90 ± 20 nm in edge length. It was clearly observed that CoS hexagonal nanostructures were highly porous mainly because of the presence of PVP as a stabilizer [29]. Detailed structural analysis of CoS hexagonal nanostructures reveals the existence of a set of (311) planes, each with a lattice spacing of 0.28 nm (Fig. S1C) [29–31]. Energy-dispersive X-ray (EDX) spectroscopy data (Fig. S2) confirm the existence of Co and S elements in CoS hexagonal nanostructures. After thermal annealing at 300 °C in air, PVP was removed, inducing changes in the architecture of CoS hexagonal nanostructures (Fig. S1D). Although the hexagonal nanostructures changed to irregular nanostructures, they were still anchored to the surfaces of the CNTs. The magnified TEM image reveals that irregular CoS nanostructures (70 ± 20 nm) were formed by the assembly of small CoS nanoparticles (NPs; most ~1 nm diameter) (Fig. S1E). The lattice spaces changed from 0.28 to 0.46 nm, indicating that changes in the crystalline orientation occurred during annealing (Fig. S1F) [32].

To further investigate the heat-induced changes in the crystalline structure of CNT/CoS composites, we recorded Raman (Fig. S4) and XPS spectra (Fig. S5). CNT/CoS composites exhibited four Raman peaks at 473, 517, 683, and 1308 cm^{-1}; the first three represent the Raman characteristics of CoS NPs, while the last one represents the C=C bond of CNTs. The first three peaks were assigned to E_g, F_{2g}, and A_{1g} modes of CoS materials, respectively [33]. The first three peaks slightly shifted and their intensities changed after annealing at 300 °C, supporting that most of CNT/CoS composites remained after annealing. We also conducted XPS analysis to support our conjecture. The data reveal that only a slight difference occurred in the binding energy of Co_{2P}, but apparent changes occurred in the binding energy of S_{2P} and S_{2S} before and after annealing at 300 °C, indicating that the formation of different crystalline orientation was due to the loss of some of S atoms (Fig. S1F).

CV measurements were conducted to evaluate the electrochemical characteristics and quantify the specific capacitance of CNT/CoS composite electrodes that had been fabricated with and without annealing at 300 °C for 0.5 h (Fig. 1A). Clearly, the annealed CNT/CoS composite electrodes yielded higher currents. According

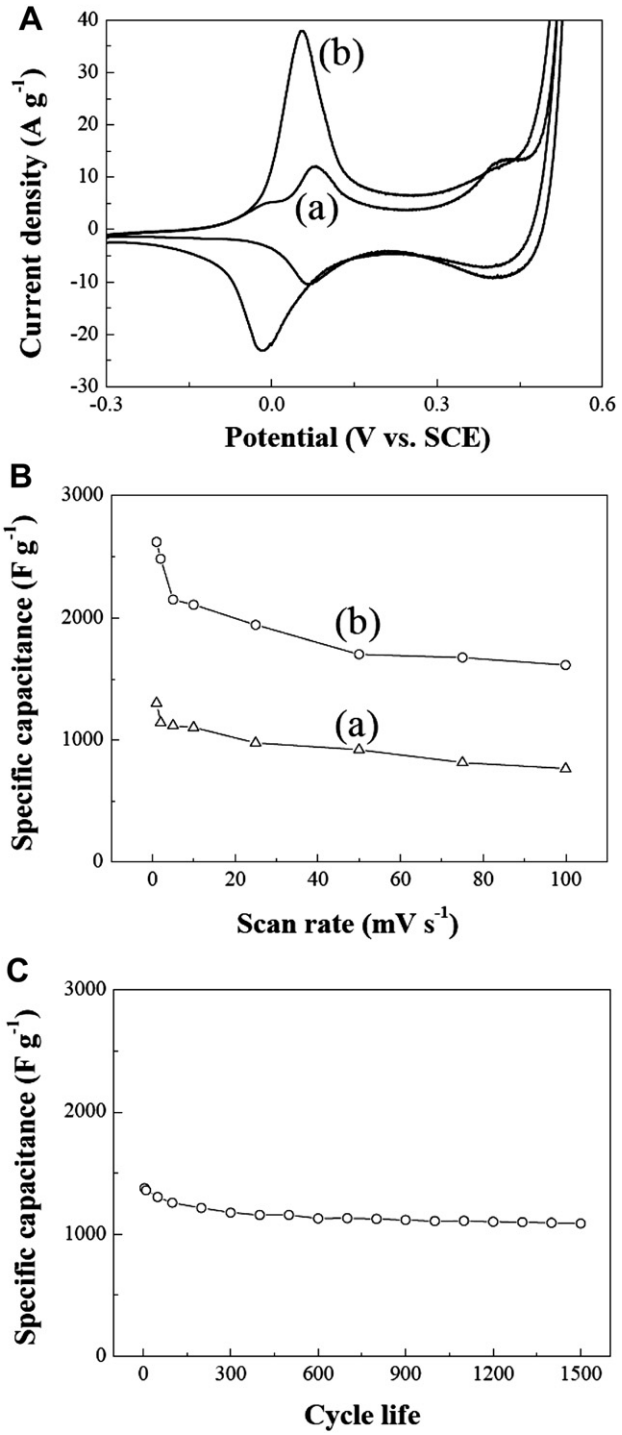

Fig. 1. (A) CV curves and (B) specific capacitance values at different scan rates of CNT/CoS composite electrodes before (a) and after (b) annealing at 300 °C for 0.5 h, respectively. (C) Cycle life of CNT/Co_3S_4 composite electrodes after annealing at 300 °C for 0.5 h.

to the literature, two plausible reactions are proposed for electrochemical reactions [6].

$$CoS + OH^- \rightleftharpoons CoSOH + H_2O + e^- \quad (1)$$

$$CoSOH + OH^- \rightleftharpoons CoSO + H_2O + e^- \quad (2)$$

The CV measurements of CNTs revealed that the current density was only ca. −0.17 A g^{-1} at 0.06 V (vs SCE), much smaller than that of the CNT/CoS composite electrode (−3.6 A g^{-1} at 0.06 V vs. SCE) (Fig. S5). The results reveal that not CNTs alone but CNT/CoS composites were responsible for the electrochemical response [6,34,35].

The current densities of the cathodic peaks at the potential 0–0.1 V were used to calculate the specific capacitance (C) of the as-prepared CNT/CoS composite electrodes from Eq. (3) [36]:

$$C = i/[m \times v], \quad (3)$$

where i is the current (A), m is the mass (g) of CNT/CoS NMs on the electrodes, and v is the scan rate (10 mV s^{-1}). The values of specific capacitance for three CNT/CoS composite electrodes that had been fabricated with and without annealing at 300 °C for 0.5 h were 2140 ± 90 and 1120 ± 80 F g^{-1}, respectively. Table 1 summarizes some recently reported SCs; on comparison of these values, our CNT/CoS composite electrodes after annealing possess a higher value of specific capacitance. To the best of our knowledge, this is the first example showing that the specific capacitance of SCs was enhanced significantly by simple annealing.

From the viewpoint of high-power applications, high-rate capability of SCs is an important parameter [24,37,38]. We thus measured the rate capabilities of CNT/CoS composite electrodes that had been fabricated with and without annealing at 300 °C at scan rates ranging from 1 to 100 mV s^{-1}. Their specific capacity values decreased approximately to 38% and 41%, respectively, upon increasing the scan rate from 1 to 100 mV s^{-1} (Fig. 1B). Upon increasing the scan rate, diffusion of OH^- ions at the interface of electrolyte/electrode was too slow for reactions (1) and (2), leading to decreased values of C. We point out that the specific capacitance of three annealed CNT/CoS composite electrodes was 1370 ± 50 F g^{-1} at a scan rate of 100 mV s^{-1}. Relative to CoS electrodes, the annealed CNT/CoS composite electrodes provided larger specific capacitance (1370 vs. 640 F g^{-1}), revealing that CNTs played a crucial role in determining the capacitance. The CNTs (1) provided a direct conductive path for CoS NPs owing to its high electrical conductivity, leading to a lower internal resistance and (2) facilitated the mass transfer process at the electrolyte–electrode interface because of its pore structures [23,39]. The annealed SCs are the first that provide specific capacitance over 1000 F g^{-1} at a scan rate of 100 mV s^{-1}.

Durability of the annealed CNT/CoS composite electrodes was evaluated to highlight their potential practicality [5,40]. The durability measurement of CNT/CoS composite electrodes was conducted at a scan rate of 100 mV s^{-1} over 1500 scan cycles (Fig. 1C). The specific capacitance of the annealed CNT/CoS composite electrodes decreased to 91% of the original value (1376.4 F g^{-1}) after 100 scans and remained almost constant up to 500 scans, showing

Table 1
Recently advanced SCs with high capacitances.

Material	Electrolyte	C (F g^{-1})[a]	Ref.
VN	1 M KOH in H_2O	1200	[41]
CNT/RuO_2	0.5 M H_2SO_4 in H_2O	1170	[19]
RuO_2	0.5 M H_2SO_4 in H_2O	1300	[8]
MWCNT/Co_3O_4	1 M KOH in H_2O	200	[21]
Co_3O_4	1 M KOH in H_2O	290	[42]
CNT/MnO_2	1 M $LiClO_4$ in propylene carbonate	250	[43]
MnO_2	0.1 M Na_2SO_4 in H_2O	1380	[44]
CNT/NiO_x	1 M KOH in H_2O	1701	[20]
NiO_x	7 M KOH in H_2O	696	[45]
CoS_x	6 M KOH in H_2O	470	[6]
CoS	1 M KOH in H_2O	640 ± 30	this work
CNT/CoS	1 M KOH in H_2O	1120 ± 80	this work
Annealed CNT/CoS	1 M KOH in H_2O	2140 ± 90	this work

[a] Scan rate 10 mV s^{-1}.

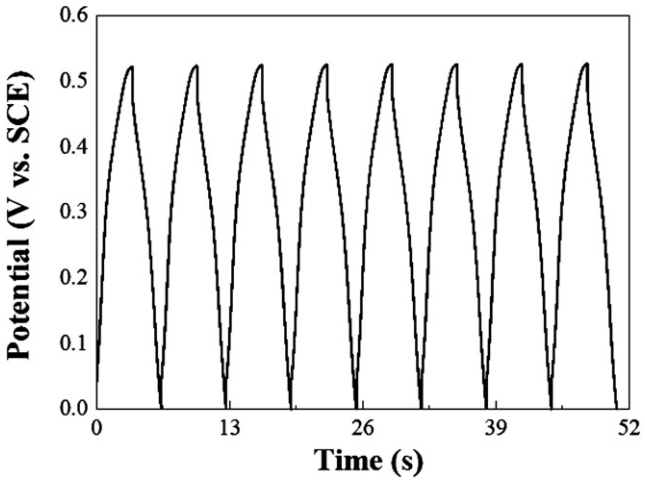

Fig. 2. Galvanostatic charge–discharge curves of the CNT/CoS composite electrodes recorded at a current density of 217.4 A g^{-1}.

good stability and long lifetime. We further conducted galvanostatic charge–discharge measurements of the annealed CNT/CoS composite electrode (Fig. 2). Because ideal high-rate SCs can provide a current density >40 A g^{-1} and a discharge time within 3 s [11–13], we conducted the measurement at a high discharge current density of 217.4 A g^{-1} or 1 mA cm^{-2} in which the mass loading of CNT/CoS composites on the electrode (area, 1 × 1 cm^2) was ca. 4.6 μg and the current was 1 mA. From the galvanostatic discharge curves, we calculated the specific capacitance (C), energy density (E), and power density (P) of CNT/CoS composite electrodes according to Eqs. (4)–(6) [7,40]:

$$C = i \times \Delta t/(\Delta V \times m) \quad (4)$$

$$E = 0.5C(\Delta V)^2/3.6 \quad (5)$$

$$P = E/\Delta t, \quad (6)$$

where i is the discharge current (A), Δt is discharge time (s), ΔV is the potential drop (V) during discharge after the internal resistance (iR) drop, and m is the mass (g) of CNT/CoS on the electrode. The values of C, E, and P were calculated to be 1332.8 F g^{-1}, 50.2 W h kg^{-1}, and 62.4 kW kg^{-1}, respectively, at a constant discharge current density of 217.4 A g^{-1}. Notably, the CNT/CoS composite electrodes provided a higher value of P (15 kW kg^{-1}) that is set by the power target of the Partnership for New-Generation of Vehicles at a fast power delivery rate (discharge time: <3 s) [11–13]. The current density of a symmetric SC at a scan rate of 10 mV s^{-1} in the CV curve (Fig. S6A) was higher than that of a single cell (Fig. 1A). From the galvanostatic charge–discharge curves (Fig. S6B), the values of specific capacitance, energy density, and power density were calculated to be 3631.5 F g^{-1}, 126.1 W h kg^{-1}, and 75.5 kW kg^{-1}, respectively, at a constant discharge current density of 1087.2 A g^{-1}. Our results clearly show that CNT/CoS NMs are excellent nanomaterials for fabrication of high-rate and high-efficiency SCs.

4. Conclusions

We have prepared high-rate and high-efficiency CNT/CoS composite electrodes. The preparation of such low-cost CNT/CoS composite electrodes is simple and reproducible. Annealing is a simple and efficient way to improve the capacitance of CNT/CoS composite electrodes. The annealed CNT/CoS composite electrodes provided extremely high values of specific capacitance, >2000 and >1000 F g^{-1} at scan rates of 10 and 100 mV s^{-1}, respectively. Relative to previous SCs, [6,8,19–21,41–45], CNT/CoS composite electrodes in this work provide greater power density and higher capacitance.

Acknowledgment

We thank the National Science Council, Taiwan, for financial support (NSC 99-2627-M-002-016 and 99-2627-M-002-017). Z. Yang thanks National Taiwan University for a postdoctoral fellowship in the Department of Chemistry.

Appendix A. Supplementary information

Supplementary data related to this article can be found online at doi:10.1016/j.jpowsour.2012.04.075.

References

[1] P. Simon, Y. Gogotsi, Nat. Mater. 7 (2008) 845–854.
[2] R. Kötz, M. Carlen, Electrochim. Acta 45 (2000) 2483–2498.
[3] A. Burke, Electrochim. Acta 53 (2007) 1083–1091.
[4] T.-Y. Wei, C.-H. Chen, H.-C. Chien, S.-Y. Lu, C.-C. Hu, Adv. Mater. 22 (2010) 347–351.
[5] Y. Wang, Z. Shi, Y. Huang, Y. Ma, C. Wang, M. Chen, Y. Chen, J. Phys. Chem. C 113 (2009) 13103–13107.
[6] F. Tao, Y.-Q. Zhao, G.-Q. Zhang, H.-L. Li, Electrochem. Commun. 9 (2007) 1282–1287.
[7] M. Kaempgen, C.K. Chan, J. Ma, Y. Cui, G. Gruner, Nano Lett. 9 (2009) 1872–1876.
[8] W. Sugimoto, H. Iwata, Y. Yasunaga, Y. Murakami, Y. Takasu, Angew. Chem. Int. Ed. 42 (2003) 4092–4096.
[9] C.-C. Hu, K.-H. Chang, M.-C. Lin, Y.-T. Wu, Nano Lett. 6 (2006) 2690–2695.
[10] J.P. Zheng, T.R. Jow, J. Power Sources 62 (1996) 155–159.
[11] D.-W. Wang, F. Li, M. Liu, G.Q. Lu, H.-M. Cheng, Angew. Chem. Int. Ed. 47 (2008) 373–376.
[12] B. Scrosati, Nature 373 (1995) 557–558.
[13] R.F. Nelson, J. Power Sources 91 (2000) 2–26.
[14] A.L.M. Reddy, M.M. Shaijumon, S.R. Gowda, P.M. Ajayan, J. Phys. Chem. C 114 (2010) 658–663.
[15] X. Du, C. Wang, M. Chen, Y. Jiao, J. Wang, J. Phys. Chem. C 113 (2009) 2643–2646.
[16] P. Lin, Q. She, B. Hong, X. Liu, Y. Shi, Z. Shi, M. Zheng, Q. Dong, J. Electrochem. Soc. 157 (2010) A818–A823.
[17] J. Liu, J. Essner, J. Li, Chem. Mater. 22 (2010) 5022–5030.
[18] K.-W. Nam, E.-S. Lee, J.-H. Kim, Y.-H. Lee, K.-B. Kim, J. Electrochem. Soc. 152 (2005) A2123–A2129.
[19] I.-H. Kim, J.-H. Kim, K.-B. Kim, Electrochem. Solid-State Lett. 8 (2005) A369–A372.
[20] K.-W. Nam, K.-H. Kim, E.-S. Lee, W.-S. Yoon, X.-Q. Yang, K.-B. Kim, J. Power Sources 182 (2008) 642–652.
[21] Y. Shan, L. Gao, Mater. Chem. Phys. 103 (2007) 206–210.
[22] S.-B. Ma, K.-Y. Ahn, E.-S. Lee, K.-H. Oh, K.-B. Kim, Carbon 45 (2007) 375–382.
[23] J. Yan, Z. Fan, T. Wei, J. Cheng, B. Shao, K. Wang, L. Song, M. Zhang, J. Power Sources 194 (2009) 1202–1207.
[24] Y. Liang, M.G. Schwab, L. Zhi, E. Mugnaioli, U. Kolb, X. Feng, K. Mullen, J. Am. Chem. Soc. 132 (2010) 15030–15037.
[25] H.C. Choi, M. Shim, S. Bangsaruntip, H. Dai, J. Am. Chem. Soc. 124 (2002) 9058–9059.
[26] S. Banerjee, S.S. Wong, Nano Lett. 2 (2002) 195–200.
[27] Z. Liu, X. Lin, J.Y. Lee, W. Zhang, M. Han, L.M. Gan, Langmuir 18 (2002) 4054–4060.
[28] L. Qu, L. Dai, E. Osawa, J. Am. Chem. Soc. 128 (2006) 5523–5532.
[29] Z. Yang, C.-Y. Chen, H.-T. Chang, J. Power Sources 196 (2011) 7874–7877.
[30] S.-J. Bao, Y. Li, C.M. Li, Q. Bao, Q. Lu, J. Guo, Cryst. Growth Des. 8 (2008) 3745–3749.
[31] Y. Yin, C.K. Erdonmez, A. Cabot, S. Hughes, A.P. Alivisatos, Adv. Funct. Mater. 16 (2006) 1389–1399.
[32] J.D. Hanawalt, H.W. Rinn, L.K. Frevel, Ind. Eng. Chem. Anal. Ed. 10 (1938) 457–512.
[33] V.G. Hadjiev, M.N. Lliev, I.V. Vergilov, J. Phys. C: Solid State Phys. 21 (1988) L199.
[34] S.-J. Bao, C.M. Li, C.-X. Guo, Y. Qiao, J. Power Sources 180 (2008) 676–681.
[35] P. Justin, G.R. Rao, Int. J. Hydrogen Energy 35 (2010) 9709–9715.
[36] M.D. Stoller, S. Park, Y. Zhu, J. An, R.S. Ruoff, Nano Lett. 8 (2008) 3498–3502.
[37] N. Li, C.R. Martin, B. Scrosati, Electrochem. Solid-State Lett. 3 (2000) 316–318.

[38] H. Zhang, G. Cao, Z. Wang, Y. Yang, Z. Shi, Z. Gu, Nano Lett. 8 (2008) 2664–2668.
[39] H. Pan, J. Li, Y.P. Feng, Nanoscale Res. Lett. 5 (2010) 654–668.
[40] Y. Xue, Y. Chen, M.-L. Zhang, Y.-D. Yan, Mater. Lett. 62 (2008) 3884–3886.
[41] D. Choi, G.E. Blomgren, P.N. Kumta, Adv. Mater. 18 (2006) 1178–1182.
[42] C. Lin, J.A. Ritter, B.N. Popov, J. Electrochem. Soc. 145 (1998) 4097–4103.
[43] S.-B. Ma, K.-W. Nam, W.-S. Yoon, X.-Q. Yang, K.-Y. Ahn, K.-H. Oh, K.-B. Kim, J. Power Sources 178 (2008) 483–489.
[44] M. Toupin, T. Brousse, D. Bélanger, Chem. Mater. 16 (2004) 3184–3190.
[45] J. Cheng, G.-P. Cao, Y.-S. Yang, J. Power Sources 159 (2006) 734–741.